Int. J. Heat Mass Transfer. Vol. 28, No. 11, pp. 2113–2120, 1985
Printed in Great Britain

0017-9310/85 $3.00 + 0.00
Pergamon Press Ltd.

Combined forced and free convection heat transfer for fully-developed laminar flow in horizontal annuli

S. KOTAKE and N. HATTORI
Faculty of Engineering, University of Tokyo, Komaba, Meguro, Tokyo 153, Japan

(*Received* 14 *March* 1985 *and in final form* 18 *May* 1985)

Abstract—The combined forced and free convection flows in a horizontal annulus are studied numerically by examining the similarity condition of fully-developed laminar flows. The finite-difference equations obtained are solved with the quadratic upstream differencing method to stabilize the convection terms with sufficient accuracy. Two cases of the thermal boundary conditions at the wall are considered for the secondary flow; constant heat flux and constant wall temperature, which lead to an appreciable difference in the flow behavior. The numerical results of the mean Nusselt number are compared with the experiment to show a good agreement.

INTRODUCTION

COMBINED forced and free convection has received considerable attention from the thermofluid–dynamical point of view as well as the practical interest of its engineering applications, since the associated fluid motion is largely interacted with the energy equation. Much theoretical and experimental work has been published on this subject. Most of the studies have concerned heat transfer for ducted flows in circular pipes. In practice, however, many heat exchanger applications require consideration of an annular configuration. Little work has been reported on combined forced and free convection in horizontal annuli [1, 2].

Circular pipe flows have only one size parameter of radial dimension and a single thermal condition at the wall, which give an explicit definition of non-dimensional flow parameters without any alternative. The flows associated with combined convection can be featured simply with these parameters. Since annular flows have two size parameters and two thermal conditions at the walls, there is always an alternative for the non-dimensional parameter to characterize the flow behavior. In circular pipes heated with constant heat flux, the flow can be developed to have a similarity which is characterized with such non-dimensional parameters. In the case of annuli, however, the situation is complicated due to multiple definition of the flow parameters and results in more complex flows to be solved numerically.

In the present study the developed laminar flows in an annulus heated axially with constant heat fluxes are examined to obtain the similarity conditions with the pertinent dimensionless flow parameters. The governing equations of the flow are then expressed in this form of similarity and solved numerically with the finite-difference method. When convection dominates diffusion at large values of the Reynolds or Grashof number, the upstream differencing method can be used to stabilize the numerical solutions. However, it always suffers from the severe inaccuracies associated with artificial numerical diffusion introduced by the one-sided upstream differencing. The quadratic upstream differencing method is used to solve combined convection flows in an annulus numerically with high accuracy and stability, and the flow behavior is studied for a range of Grashof number under the thermal boundary conditions of constant heat flux and constant wall temperature.

FULLY-DEVELOPED FLOW AND SIMILARITY

As shown in Fig. 1, the fluid in an annulus is heated axially with uniform heat flux at the walls, having constant physical properties except the density in the buoyancy term. Integrating the equation of energy in the axial direction with respect to the cross-sectional area of the annulus gives the following relation of energy balance:

$$\frac{\mathrm{d}}{\mathrm{d}z}\int_0^{2\pi}\int_{R_i}^{R_o}\rho c w T r\,\mathrm{d}r\,\mathrm{d}\theta = 2\pi(R_o Q_o + R_i Q_i). \quad (1)$$

where w is the axial velocity component, R_o and R_i the outer and inner radius, Q_o and Q_i the heat fluxes into the fluid at the outer and inner walls, ρ the density and c the specific heat. The heat conduction in the axial direction is neglected due to its small effect compared with the axial convection. The averaged axial flow velocity $\bar{w}$ and the flow-averaged temperature $\bar{T}$ are defined, respectively, as:

$$\bar{w} = \frac{1}{\pi(R_o^2 - R_i^2)}\int_0^{2\pi}\int_{R_i}^{R_o} w r\,\mathrm{d}r\,\mathrm{d}\theta,$$
$$\bar{T} = \frac{1}{\pi(R_o^2 - R_i^2)\bar{w}}\int_0^{2\pi}\int_{R_i}^{R_o} w T r\,\mathrm{d}r\,\mathrm{d}\theta. \quad (2)$$

NOMENCLATURE

c	specific heat
g	acceleration of gravity
Gr	Grashof number
l_r	reference length of secondary flow
Nu	Nusselt number
Pr	Prandtl number
Q, q	heat flux, dimensionless heat flux
R, r	radius, dimensionless radius
T	temperature
T^*	$= T-\bar{T}$
$\bar{T}$	flow-averaged temperature
T_0	temperature without free convection
T_1	temperature due to free convection
T_r	reference temperature of secondary flow
u_r	reference velocity of secondary flow
u, v	velocity components in (r, θ)-direction
w	axial flow velocity
$\bar{w}$	mean axial flow velocity
w_0	axial velocity without free convection
w_1	axial velocity due to free convection
z	axial coordinate.

Greek symbols

β	coefficient of thermal expansion
λ	thermal conductivity
μ	dynamic viscosity
ν	kinematic viscosity
ρ	density
θ	circumferential angle
ψ	stream function
ω	vorticity.

Subscripts

i	inner wall
o	outer wall
r	reference
w	wall.

Since $\bar{w}$ is constant, equation (1) gives

$$\rho c\bar{w}\frac{\mathrm{d}\bar{T}}{\mathrm{d}z}=\frac{2(R_oQ_o+R_iQ_i)}{R_o^2-R_i^2}. \tag{3}$$

From equations (1) and (2), it is seen that the temperature should be a linear function of the axial length. When the temperature is measured from the average temperature

$$T^*=T-\bar{T} \tag{4}$$

the equation of energy for developed flows indicates that the temperature difference T^* is independent of the axial length, being a function of only r and θ.

The equations of motion for a developed flow show that the gradient of pressure should also be independent of the axial length, hence the pressure can be expressed in the form

$$p(r,\theta,z)=kz+p^*(r,\theta) \tag{5}$$

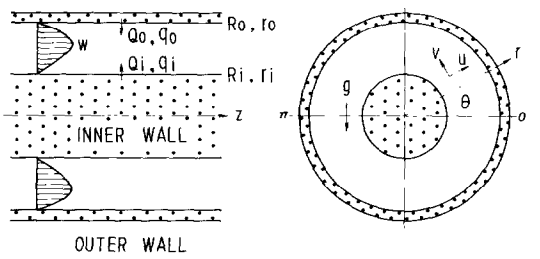

FIG. 1. Combined forced and free convection flow in a horizontal annulus.

where k is a constant. Integration of the equation of motion in the axial direction with respect to the annulus cross-section gives

$$\frac{\mathrm{d}p}{\mathrm{d}z}=k=\frac{1}{\pi(R_o^2-R_i^2)}\times\int_0^{2\pi}\left\{\left(r\frac{\partial w}{\partial r}\right)_o-\left(r\frac{\partial w}{\partial r}\right)_i\right\}\mathrm{d}\theta. \tag{6}$$

By defining the stream function and the vorticity as

$$u=\frac{\partial\psi}{r\,\partial\theta},\quad v=-\frac{\partial\psi}{\partial r},\quad \omega=\nabla^2\psi \tag{7}$$

and expressing the flow variables in a dimensionless form with their reference values (denoted with the subscript r; u_r, l_r, T_r), the equations of motion and energy for a fully-developed laminar flow can be given as

$$Re\left(u\frac{\partial\omega}{\partial r}+v\frac{\partial\omega}{r\,\partial\theta}\right)=\nabla^2\omega+\frac{Gr}{Re}\times\left(\frac{\partial T^*}{r\,\partial\theta}\sin\theta-\frac{\partial T^*}{\partial r}\cos\theta\right) \tag{8}$$

$$Re\left(u\frac{\partial w}{\partial r}+v\frac{\partial w}{r\,\partial\theta}\right)=\nabla^2w-\frac{2}{\pi(r_o^2-r_i^2)}\times\int_{-\pi/2}^{\pi/2}\left\{\left(r\frac{\partial w}{\partial r}\right)_o-\left(r\frac{\partial w}{\partial r}\right)_i\right\}\mathrm{d}\theta \tag{9}$$

$$Re\left(u\frac{\partial T^*}{\partial r}+v\frac{\partial T^*}{r\,\partial\theta}+w\frac{\partial\bar{T}}{\partial z}\right)=\frac{1}{Pr}\nabla^2T^* \tag{10}$$

$$\nabla^2\equiv\frac{\partial^2}{\partial r^2}+\frac{1}{r}\frac{\partial}{\partial r}+\frac{1}{r^2}\frac{\partial^2}{\partial\theta^2}$$

where

$$Re = \frac{\rho l_r u_r}{\mu}, \quad Gr = \frac{g\beta l_r^3 T_r}{\nu^2}, \quad Pr = \frac{\mu c}{\lambda}. \tag{11}$$

The boundary conditions are given by

$$\begin{aligned} r = (r_o, r_i): \quad & \psi = 0, \quad \omega = \frac{\partial^2 \psi}{\partial r^2}, \\ & w = 0, \quad \frac{\partial T^*}{\partial r} = (q_o, -q_i) \\ \theta = \left(\frac{\pi}{2}, -\frac{\pi}{2}\right): \quad & \psi = 0, \quad \omega = 0, \\ & \frac{\partial w}{\partial \theta} = 0, \quad \frac{\partial T^*}{\partial \theta} = 0 \end{aligned} \tag{12}$$

where the heat flux is non-dimensionalized by $\lambda T_r / l_r$.

With the heat balance relation of equation (3) in the dimensionless form, the axial heat convection in equation (10) can be rewritten as

$$w \frac{\partial \bar{T}}{\partial z} \to \frac{2}{Pr\ Re} \frac{r_o q_o + r_i q_i}{r_o^2 - r_i^2} w$$

where the axial flow velocity is normalized with the mean value $w/\bar{w} \to w$, that is

$$\int_0^{2\pi} \int_{r_i}^{r_o} wr \, dr \, d\theta = 1. \tag{13}$$

The reference values u_r, T_r and l_r can be chosen so as to satisfy the relations

$$\frac{\rho l_r u_r}{\mu} = 1 \quad \frac{r_o q_o + r_i q_i}{r_o^2 - r_i^2} = \frac{1}{2}. \tag{14}$$

In order to examine the free convection effect, it is useful to express the temperature and the axial velocity subtracted from those without free convection as

$$\begin{aligned} T^*(r, \theta) &= T_0(r) + T_1(r, \theta) \\ w(r, \theta) &= w_0(r) + w_1(r, \theta) \end{aligned} \tag{15}$$

where T_0 and w_0 are the temperature and axial velocity of developed flow with $(u, v) = 0$. The temperature for forced convection flows in an annulus can be obtained analytically by solving the energy equation

$$\frac{1}{r} \frac{d}{dr}\left(r \frac{dT_0}{dr}\right) = w_0$$

with the fully-developed axial velocity

$$w_0(r) = 2\left(r_o^2 + r_i^2 + \frac{r_o^2 - r_i^2}{\ln r_i/r_o}\right)^{-1} \times \left(r_o^2 - r^2 - \frac{r_o^2 - r_i^2}{\ln r_i/r_o} \ln r/r_o\right)$$

and the thermal boundary conditions at the walls (12).

With equations (14) and (15), the governing equations (8)–(10) are rewritten as

$$u \frac{\partial \omega}{\partial r} + v \frac{\partial \omega}{r\, \partial \theta} = \nabla^2 \omega + Gr\left(\frac{\partial T_1}{r\, \partial \theta} \sin \theta - \frac{\partial T_1}{\partial r} \cos \theta - \frac{\partial T_0}{\partial r} \cos \theta\right) \tag{16}$$

$$u \frac{\partial w_1}{\partial r} + v \frac{\partial w_1}{r\, \partial \theta} = \nabla^2 w_1 - u \frac{\partial w_0}{\partial r} - \frac{2}{\pi(r_o^2 - r_i^2)} \int_{-\pi/2}^{\pi/2} \left\{\left(r \frac{\partial w_1}{\partial r}\right)_o - \left(r \frac{\partial w_1}{\partial r}\right)_i\right\} d\theta \tag{17}$$

$$u \frac{\partial T_1}{\partial r} + v \frac{\partial T_1}{r\, \partial \theta} = \frac{1}{Pr} \nabla^2 T_1 - u \frac{\partial T_0}{\partial r} - \frac{1}{Pr} w_1 \tag{18}$$

with the boundary conditions (12) modified for temperature T_1 as

$$r = (r_o, r_i): \quad \frac{\partial T_1}{\partial r} = 0 \tag{19}$$

and

$$\begin{aligned} \int_{-\pi/2}^{\pi/2} \int_{r_i}^{r_o} w_1 r \, dr \, d\theta = 0 \\ \int_{-\pi/2}^{\pi/2} \int_{r_i}^{r_o} (w_0 T_1 + w_1 T_0 + w_1 T_1) r \, dr \, d\theta = 0. \end{aligned} \tag{20}$$

The heat transfer coefficients at the walls are

$$Nu_o(\theta) = \frac{q_o}{T_o^*} \quad Nu_i(\theta) = \frac{q_i}{T_i^*} \tag{21}$$

and their mean values based on the mean wall temperature averaged circumferentially are

$$\begin{aligned} Nu_o &= \pi q_o \left(\int_{-\pi/2}^{\pi/2} T_o^* \, d\theta\right)^{-1} \\ Nu_i &= \pi q_i \left(\int_{-\pi/2}^{\pi/2} T_i^* \, d\theta\right)^{-1}. \end{aligned} \tag{22}$$

The thermal boundary condition of equation (19) is of the Neuman type and the absolute values of temperature should be determined by the restrictive condition, equation (20). This is not favorable to the computational stability. As an alternative method, the wall temperature may be assumed to be circumferentially constant, which is specified so as to satisfy equation (20). Such an approximation can be expected for annulus walls of high-conductivity materials. The thermal condition at the wall is then

$$r = (r_o, r_i): \quad T_1 = 0 \tag{23}$$

and the heat transfer coefficient is given by

$$\begin{aligned} Nu(\theta) &= \frac{1}{T_w^*} \left(\frac{\partial T^*}{\partial r}\right)_w \\ Nu &= \frac{1}{\pi T_w^*} \int_{-\pi/2}^{\pi/2} \left(\frac{\partial T^*}{\partial r}\right)_w d\theta. \end{aligned} \tag{24}$$

NUMERICAL METHOD

With the finite-difference method, the governing equations (16)–(18) can be solved under the boundary conditions (12) with (19) for the case of constant heat flux or with (23) for the case of constant wall temperature. The diffusion terms can be replaced by central finite differences which have the second-order accuracy of truncation error. For the convection terms, central differencing can be also used to retain errors of the second order, but it always yields stability problems at higher Reynolds or Grashof numbers. In order to suppress such an instability of computation, one-sided upstream differencing may be employed;

$$u\frac{\partial\omega}{\partial r} = u_i\frac{\omega_+ - \omega_-}{\Delta r} \tag{25}$$

$$u_i > 0: \quad \omega_+ = \omega_i, \quad \omega_- = \omega_{i-1}$$

$$u_i < 0: \quad \omega_+ = \omega_{i+1}, \quad \omega_- = \omega_i$$

where the subscript i means the value at $r = i\,\Delta r$. Although this upwind method proves higher stabilities, it suffers from severe inaccuracies due to its artificial numerical diffusion terms introduced implicitly. In the present study, after examining several methods to solve such problems of stability and accuracy, the quadratic upstream differencing method is employed for the convection terms, in which the linear interpolation is corrected by a term proportional to the three-point upstream weighted value with a quadratic function [3]

$$u\frac{\partial\omega}{\partial r} = u_i\frac{\omega_+ - \omega_-}{\Delta r} \tag{26}$$

$u_i > 0$:

$$\omega_+ = \tfrac{1}{2}(\omega_{i+1}+\omega_i) - \tfrac{1}{8}(\omega_{i+1}+\omega_{i-1}-2\omega_i)$$

$$\omega_- = \tfrac{1}{2}(\omega_i+\omega_{i-1}) - \tfrac{1}{8}(\omega_i+\omega_{i-2}-2\omega_{i-1})$$

$u_i < 0$:

$$\omega_+ = \tfrac{1}{2}(\omega_{i+1}+\omega_i) - \tfrac{1}{8}(\omega_i+\omega_{i+2}-2\omega_{i+1})$$

$$\omega_- = \tfrac{1}{2}(\omega_i+\omega_{i-1}) - \tfrac{1}{8}(\omega_{i+1}+\omega_{i-1}-2\omega_i).$$

At points next to the wall where the quadratic upstream differencing is not applied, central differencing or linear upstream differencing can be used since the convection terms are not appreciable there.

The finite-difference equations are then solved time-step-wise as for unsteady equations to obtain the steady equations. Initially, computation is started at sufficiently small values of the Grashof number (about 10^3) at which the buoyancy effect is hardly recognized, and continued to larger values of the Grashof number successively by using the preceding result as the initial condition of the next step. The used mesh sizes are $\Delta r^{-1} = 40$–80 and $\Delta\theta^{-1} = 60$–120 owing to the Grashof number 10^3–10^6.

In the following numerical computation, the solutions with the linear upstream differencing method begin to oscillate at the Grashof number about 10^4, and they burst to diverge at Grashof numbers above 10^5. The quadratic upstream differencing method, however, is proved to obtain the solution converged even at Grashof numbers higher than 10^6. The number of iterations required to reach a steady solution is increased with the Grashof number from 10^2 to 10^4. At $Gr = 10^7$, it cannot also succeed in giving a converged solution. Convergence is ascertained by the relative error criterion at each point

$$\max\{|(\psi^{n+1}-\psi^n)/\psi^n|, |(T_1^{n+1}-T_1^n)/T_1^n|\} < 10^{-4}$$

where the superscript n means the nth step of iteration.

NUMERICAL RESULTS AND DISCUSSIONS

In Fig. 2 streamlines $\psi/\psi_{\max}$ and isotherms $T_1/T_{1\max}$ are shown for an annulus of $r_o = 1$ and $r_i = 0.5$ at the Grashof number 10^4–10^6 and $Pr = 1$ for the case of (a) inner wall heated ($q_i = 1$, $q_o = 0$) and (b) outer wall heated uniformly ($q_o = 1$, $q_i = 0$). Wall temperature increments T_1 are shown in Fig. 3. It is seen from Fig. 2 that in both cases the secondary flows associated with free convection behave so as to reduce temperature difference in the annulus. In the case of inner wall heated, the fluid flows up along the inner wall to form vortices having their center in the upper part of the annulus. The vortex strength increases with the Grashof number, and finally the vortex breaks up into two or more vortices. When the outer wall is heated, the associated vortex flows have their center in the lower annulus, and also increase their strength with the Grashof number. At small Grashof numbers, the vortex circulation is stronger in the case of outer wall heating, but at larger Grashof numbers it is increased much more in the case of inner wall heating. From Fig. 3, it is seen that the wall temperature is reduced at the lower part and increased at the upper part. Differences in the wall-temperature increments at the outer and inner walls are remarkable at the upper part in the case of inner wall heating and at the lower part in the case of outer wall heating. As the Grashof number is increased, the differences are reduced in the case of outer wall heating and enhanced in the case of inner wall heating.

By using equations (19) or (23), the thermal boundary conditions of the secondary flow are changed from uniform heat fluxes through the walls to constant wall temperatures. In Fig. 4, the latter flows associated are presented. In comparison with Fig. 2, remarkable changes in the isotherms and streamlines can be observed. It should be noted that the thermal boundary conditions have a considerable effect on the secondary flow behavior. In the case of outer wall heated, since reduction in the wall temperature is not allowed at the outer wall as seen in Fig. 3(b), it keeps the temperature gradient favorable to the buoyancy force even at the upper part of annulus hence forming a strong vortex centered in the upper annulus. On the other hand, flows with constant heat flux cause unfavorable temperature gradients at the upper annulus to the buoyancy effect and form less strong vortices confined in the lower

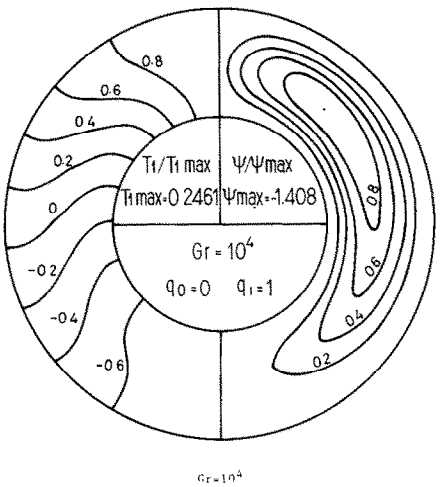

Gr=10⁴

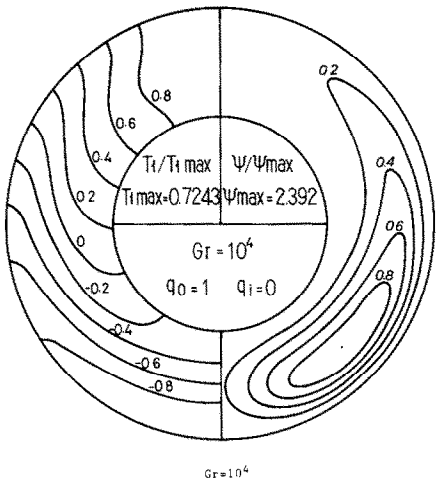

Gr=10⁴

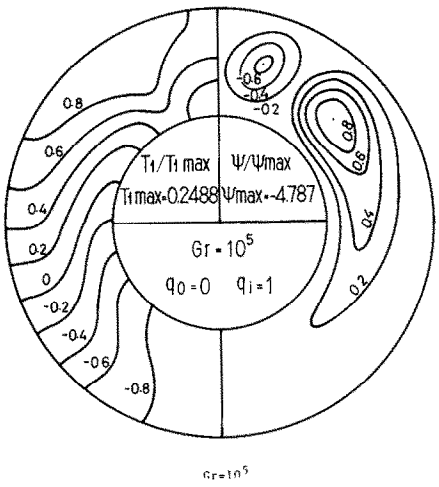

Gr=10⁵

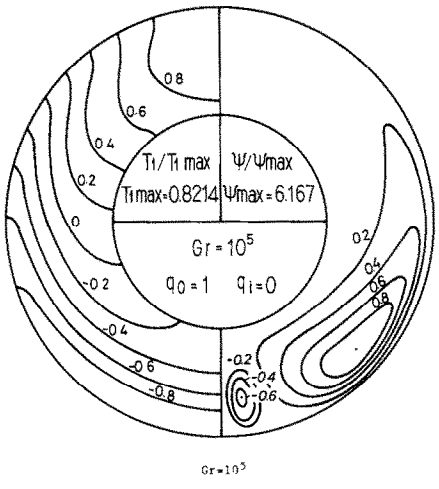

Gr=10⁵

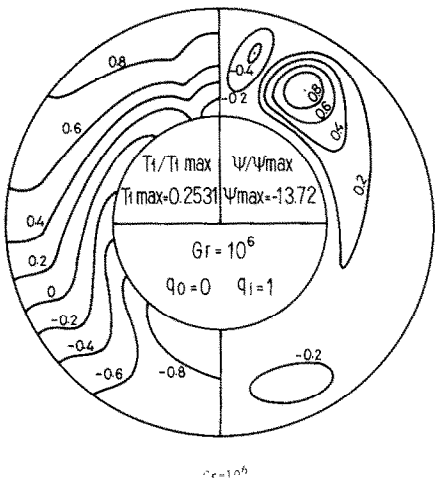

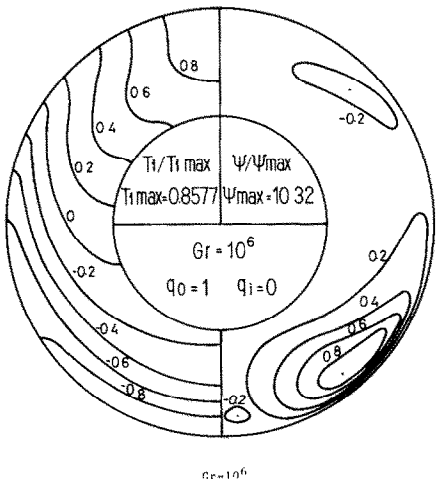

Gr=10⁶

FIG. 2(a). Streamlines and isotherms: inner wall heating.

FIG. 2(b). Streamlines and isotherms: outer wall heating.

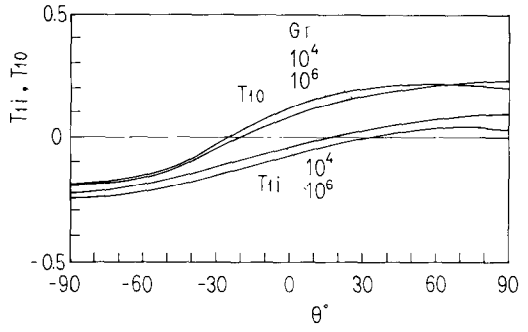

FIG. 3(a). Wall temperature distributions: inner wall heating.

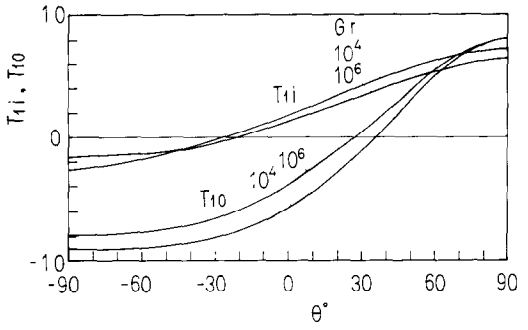

FIG. 3(b). Wall temperature distributions: outer wall heating.

region. In the case of inner wall heating, the restriction of wall temperature at the inner wall also tends to make an increase in the vortex strength, but it is not so remarkable as in the case of outer wall heating except for the number of vortices associated.

In order to compare the numerical results with the experiment, the reference values of u_r, T_r and l_r should be specified. These values must satisfy equations (14). Another relation remains arbitrary to be imposed. As the relation, three cases may be considered such as

$$\text{(I)} \quad Q_r = \lambda T_r/l_r = Q_o + Q_i$$

$$\text{(II)} \quad l_r = R_o - R_i$$

$$\text{(III)} \quad T_r = (R_o Q_o + R_i Q_i)/\lambda$$

with which equation (14) gives the reference values (Table 1). In ref. [2], a number of experiments carried out for a range of the Grashof number, the ratio R_o/R_i and heat fluxes Q_o and Q_i. The results shows that the case (I) gives the best correlation concerning the relationship between the mean Nusselt number and the Grashof number. In Fig. 5, the Nusselt numbers obtained numerically are compared with those of the experiment (in ref. [2], $Gr_{exp} = 4^4 Gr_{cal}$, $Nu_{exp} = 4Nu_{cal}$). The Nusselt numbers calculated are slightly higher than the experiment, especially at small Grashof numbers. The results obtained with the thermal condition of constant wall temperature deviate much more from the experiment. The approximate thermal

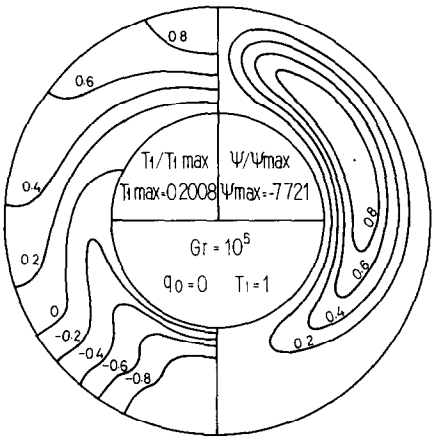

FIG. 4(a). Streamlines and isotherms for cases of constant wall temperature: inner wall heating.

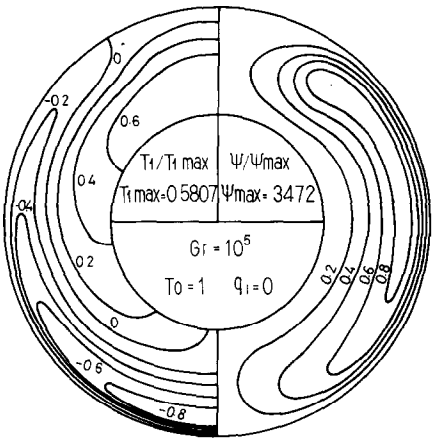

FIG. 4(b). Streamlines and isotherms for cases of constant wall temperature: outer wall heating.

condition should be thus carefully applied even to the integrated features of flow such as the mean heat transfer coefficient.

CONCLUSION

Examining the similarity condition of fully-developed laminar flows in a horizontal annulus, the combined forced and free convection flows are studied numerically. With appropriate reference values, the governing equations can be expressed in a dimensionless form with a Grashof number. As for the thermal boundary conditions of the secondary flow, two cases of constant heat fluxes and constant wall temperatures are considered. The governing equations obtained are solved numerically with the quadratic upstream differencing method to stabilize the computation with sufficient accuracy. With the numerical results, the flow features of combined forced and free convection in the annulus are studied. The vortex associated increases its

Table 1. Characteristic reference values

	Case I (Q_r)	Case II (l_r)	Case III (T_r)
l_r	$\Delta R^2 \frac{Q}{\overline{RQ}}$	ΔR	$(\Delta R^2)^{1/2}$
u_r	$\frac{\nu}{\Delta R^2}\frac{\overline{RQ}}{Q}$	$\frac{\nu}{\Delta R}$	$\frac{\nu}{(\Delta R^2)^{1/2}}$
T_r	$\frac{Q^2}{\lambda}\frac{\Delta R^2}{\overline{RQ}}$	$\frac{\overline{RQ}}{\lambda}\frac{\Delta R}{R}$	$\frac{\overline{RQ}}{\lambda}$
Q_r	Q	$\frac{\overline{RQ}}{R}$	$\frac{\overline{RQ}}{(\Delta R^2)^{1/2}}$
Gr	$\frac{g\beta Q}{\lambda\nu^2}\left(\Delta R^2\frac{Q}{\overline{RQ}}\right)^4$	$\frac{g\beta}{\lambda\nu^2}\frac{\overline{RQ}}{R}(\Delta R)^4$	$\frac{g\beta\overline{RQ}}{\lambda\nu^2}(\Delta R^2)^{3/2}$
Nu	$\frac{h}{\lambda}\frac{\Delta R^2 Q}{\overline{RQ}}$	$\frac{h}{\lambda}\Delta R$	$\frac{h}{\lambda}(\Delta R^2)^{1/2}$

$$R \equiv (R_o + R_i)/2 \quad \Delta R \equiv R_o - R_i \quad \Delta R^2 \equiv \Delta R \cdot R$$
$$Q \equiv Q_o + Q_i \quad \overline{RQ} \equiv R_o Q_o + R_i Q_i.$$

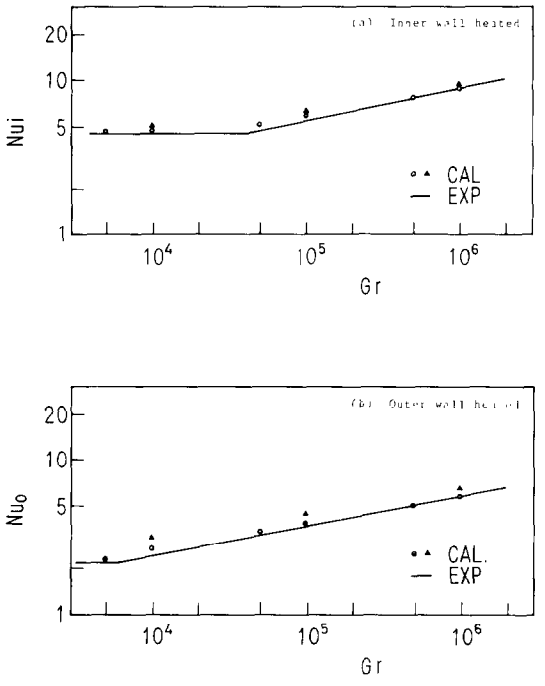

FIG. 5. Mean Nusselt number compared with experiments (Pr = 1). —— Experiment (ref. [2]); ○ calculation with constant heat flux; △ calculation with constant wall temperature. (a) Inner wall heating; (b) outer wall heating.

strength with the Grashof number, especially more rapidly in the case of inner wall heating, acting so as to reduce the temperature difference. The thermal boundary conditions at the wall lead to a remarkable difference in the flow behavior. The condition of constant wall temperature which restricts the change in the wall temperature alleviates reduction in the temperature difference and causes strong vortex circulations, especially in the case of outer wall heating. The numerical results of the mean Nusselt number are compared with the experiment to show a good agreement. The thermal boundary condition of constant wall temperature gives larger values of the mean Nusselt number than those for the case of constant heat flux.

REFERENCES

1. J. Heutz and J. P. Petit, Natural and mixed convection in concentric annular space—experimental and theoretical results for liquid metals, *Proc. 5th Int. Heat Transfer Conference*, Vol. 3, p. 169 (1974).
2. N. Hattori and S. Kotake, Combined free and forced convection heat-transfer for fully developed laminar flow in horizontal tubes (experiments), *Trans. Japan Soc. mech. Engrs*, **43**, 3379 (1977).
3. B. P. Leonard, A stable and accurate convective modeling procedure based on quadratic upstream interpolation, *Comput. meth. appl. Mech. Engng* **19**, 59–98 (1979).

CONVECTION MIXTE THERMIQUE POUR UN ECOULEMENT LAMINAIRE ETABLI DANS UN ESPACE ANNULAIRE HORIZONTAL

Résumé—Les écoulements de convection mixte dans un espace annulaire horizontal sont étudiés numériquement en examinant la condition de similarité des écoulements laminaires pleinement établis. Les équations aux différences finies obtenues sont résolues par la méthode de différenciation quadratique pour stabiliser les termes de convection avec une précision suffisante. Deux cas de conditions aux limites thermiques à la paroi sont considérés pour l'écoulement secondaire, flux thermique constant et température parietale constante, ce qui conduit à une différence appréciable dans le comportement de l'écoulement. Les résultats numériques du nombre de Nusselt moyen sont comparés avec l'expérience pour montrer un bon accord.

WÄRMEÜBERGANG BEI MISCH-KONVEKTION IN EINER VOLLAUSGEBILDETEN LAMINARSTRÖMUNG IN HORIZONTALEN RINGRÄUMEN

Zusammenfassung—Überlagerte erzwungene und freie Konvektionsströmungen in einem horizontalen Ringraum werden numerisch untersucht, indem die Ähnlichkeitsbedingungen der voll ausgebildeten Laminarströmungen überprüft werden. Die Finiten-Differenzen-Gleichungen werden mit dem quadratischen Rückwärts-Differenzen-Verfahren gelöst, um die Konvektionsterme mit ausreichender Genauigkeit stabilisieren zu können. Zwei thermische Randbedingungen an der Wand werden für die Sekundärströmung betrachtet: konstante Wärmestromdichte und konstante Wandtemperatur. Dies führt zu einem wahrnehmbaren Unterschied im Strömungsverhalten. Die numerischen Ergebnisse der mittleren Nusseltzahl werden mit Experimenten verglichen und zeigen gute Übereinstimmung.

ТЕПЛООБМЕН ПРИ СМЕШАННОЙ СВОБОДНОЙ И ВЫНУЖДЕННОЙ КОНВЕКЦИИ ДЛЯ ПОЛНОСТЬЮ РАЗВИТОГО ЛАМИНАРНОГО ТЕЧЕНИЯ В ГОРИЗОНТАЛЬНЫХ КОЛЬЦЕВЫХ КАНАЛАХ

Аннотация—Смешанная свободная и вынужденная конвекция при полностью развитом ламинарном течении в горизонтальном кольцевом канале исследована численно для автомодельных условий. Полученные конечно-разностные уравнения решались методом, обеспечивающим с достаточной точностью стабилизацию конвективных членов. Вторичные течения рассмотрены для двух случаев тепловых граничных условий на стенке: постоянном тепловом потоке и постоянной температуре стенки, которые приводят к значительным различиям в поведении потока. Показано хорошее соответствие численных результатов для среднего числа Нуссельта с экспериментальными данными.